

# Merging Experimental Study of High-Beta ST Formation for Non-Inductive Plasma Start-Up Assisted by NBI in TS-4

Keii GI, Toru II<sup>1)</sup>, Toshiyuki UMEZAWA, Michiaki INOMOTO and Yasushi ONO

*Graduate School of Frontier Sciences, The University of Tokyo, Chiba 277-8561, Japan*

<sup>1)</sup>*Graduate School of Engineering, The University of Tokyo, Tokyo 113-8656, Japan*

(Received 14 November 2012 / Accepted 18 February 2013)

Spherical tokamak (ST) merging start-up for high-beta ST formation was developed in the TS-4 merging/reconnection experiment under a high external toroidal magnetic field. We optimized the formation of a stable high-beta ST ( $\beta_t > 30\%$ ) by adjusting the initial parameters of two low-beta STs. We precisely analyzed the produced high-beta STs by MEUDAS using the measured and fitted profiles, and found that they exhibited low-plasma internal inductance because of a hollow current profile, a paramagnetic toroidal field, and weakly reversed shear. A pressure-driven instability analysis indicates that the merging STs become unstable when their  $q$ -values are less than 1. In the first high-power neutral beam injection experiment (#1 and #2,  $P_{\text{NBI}} \sim 0.4$  MW) in TS-4, the decay time and magnetic flux of the produced STs were improved, mainly because of pre-ionization and merging/reconnection effects.

© 2013 The Japan Society of Plasma Science and Nuclear Fusion Research

Keywords: ST, non-inductive start-up, plasma merging, magnetic reconnection, high-beta, NBI, MHD equilibrium reconstruction, pressure-driven instability

DOI: 10.1585/pfr.8.1402023

## 1. Introduction

Non-inductive plasma start-up is crucial for spherical tokamak (ST) fusion reactors because of their narrow space for the center solenoid (CS) coils. The plasma merging method [1], which has been developed in TS-3, TS-4, UTST, and MAST, is a promising candidate for non-inductively producing a high-beta ST within a short reconnection time. The TS-4 merging experiment has been developing the first merging start-up of a stable high-beta ST by changing the initial parameters of two low-beta STs under a high-external toroidal magnetic field compared with conventional ones ( $\sim 0.1$  T) [2]. We used the experimentally measured profiles to reconstruct the magnetohydrodynamic (MHD) equilibria and analyzed the pressure-driven instabilities (the ideal interchange mode and ideal ballooning mode) using the MEUDAS code [3]. The first result of neutral beam injection (NBI) to ST plasma is presented in this study.

## 2. TS-4 ST Merging Experiment

In the TS-4 ST merging experiment, two low-beta ( $\beta \sim 10\%$ ) STs with parallel plasma currents were individually created by the flux cores, which have poloidal and toroidal magnetic field (PF and TF, respectively) coils inside, as shown in Fig. 1 (a) and Fig. 2 (a). They were compressed by the PF coils and merged on the mid-plane ( $z = 0$ ) through magnetic reconnection, causing significant ion heating [4] and relaxation to new high-beta ( $\beta \sim 40\%$ )

ST plasma.

A two-dimensional (2-D) ( $10 \times 9$ ) array of magnetic probes was located on the  $R$ - $Z$  plane in the cylindrical vac-

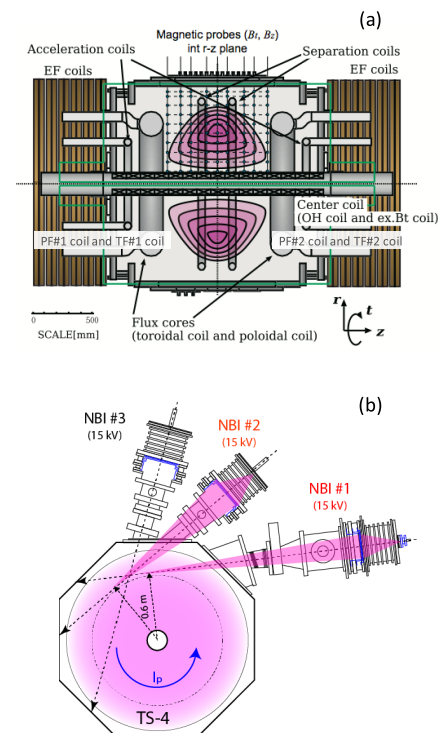


Fig. 1 Schematic views of (a) TS-4 merging device and (b) three NBI devices installed on TS-4.

author's e-mail: gi@ts.t.u-tokyo.ac.jp

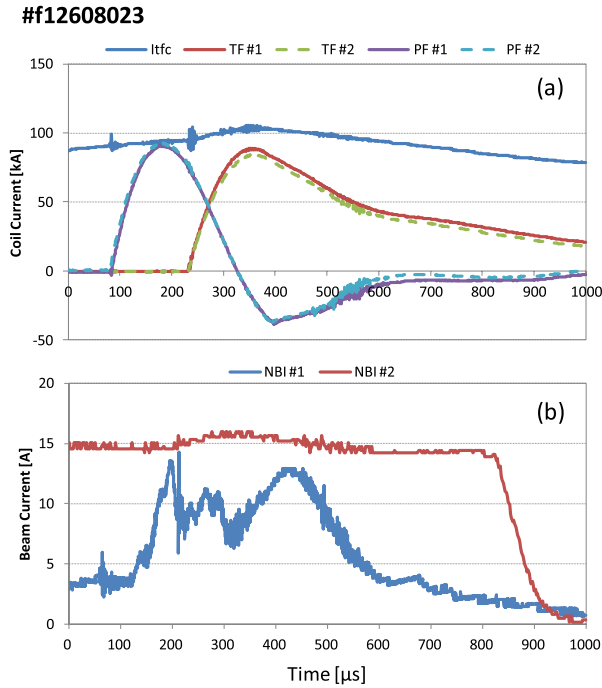


Fig. 2 Waveforms of (a) TS-4 coil currents and (b) beam currents of NBI #1 and #2 for  $V_{PF} = 5.5$  kV and  $I_{tfc} = 80$  kA. A DC power supply was used for the EF coils of  $I_{EF} = 240$  A.

uum vessel of TS-4 to measure the poloidal and toroidal magnetic fields  $B_z$  and  $B_t$ , respectively. They were used to calculate the magnetic fields, poloidal flux  $\Psi$ , poloidal and toroidal current densities  $j_z$  and  $j_t$ , respectively, and plasma current  $I_p$ . The thermal pressure function  $P(\Psi)$  and the poloidal current function  $F(\Psi)$  at the magnetic flux surfaces were also calculated by the least-squares fitting method.

Three Co-NB injectors were installed on TS-4, as shown in Fig. 1 (b). A washer gun source was used for NBI #1 [5], and filament sources were used for NBI #2 and #3. As shown in Fig. 2 (b), the NBI power was maintained throughout ST formation. In this experiment, the charged voltage of the PF coils in the flux cores ( $V_{PF}$ ) and the external TF coil current ( $I_{tfc}$ ) were varied to evaluate how the parameters of the two initial STs affect the merging formation of high-beta STs. NBI #1 and #2, with a total power of  $P_{NBI} \sim 0.4$  MW, were synchronously operated for the first time in TS-4 ST experiments.

Figure 3 shows the time evolutions of (a) the poloidal flux  $\Psi$  and (b) the plasma current  $I_p$  of the merging STs produced by  $V_{PF} = 5.5$  or  $6.0$  kV,  $I_{tfc} = 80$  or  $100$  kA, w/o NBI, and the single ST (no merging) for  $V_{PF} = 5.5$  kV and  $I_{tfc} = 80$  kA without NBI. Figure 3 (c) shows the time evolution of the poloidal flux  $\Psi$  on the  $R$ - $Z$  plane (lines and colors) of the merging ST produced for  $V_{PF} = 5.5$  kV and  $I_{tfc} = 80$  kA without NBI. The larger of the two poloidal fluxes was used before merging in Fig. 3 (a). Because we did not use ohmic heating by the CS coils in the exper-

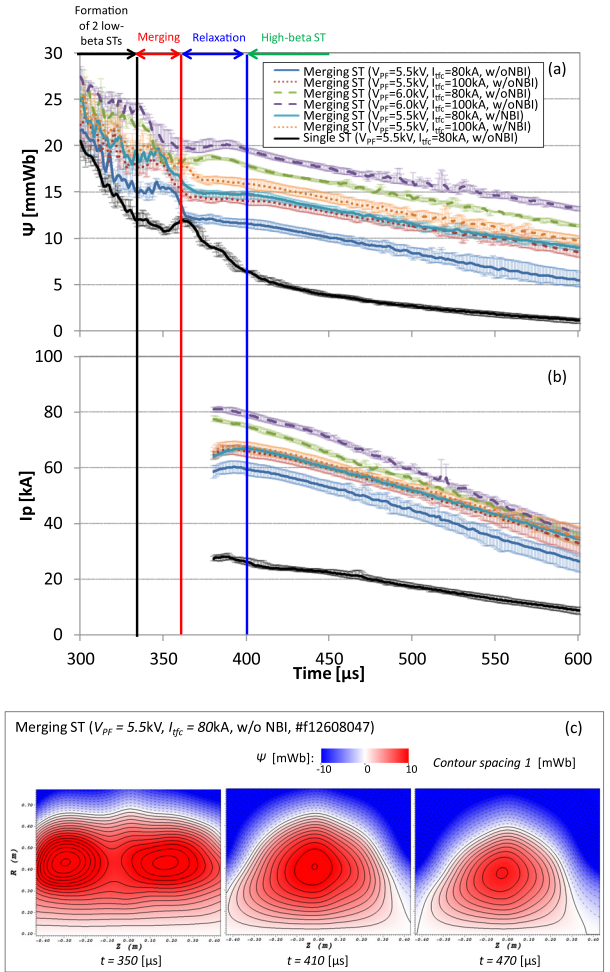


Fig. 3 Time evolutions of (a) poloidal flux  $\Psi$  and (b) plasma current  $I_p$  of the merging STs w/o NBI for  $V_{PF} = 5.5/6.0$  kV,  $I_{tfc} = 80/100$  kA, and those of the single ST (no merging) for  $V_{PF} = 5.5$  kV and  $I_{tfc} = 80$  kA without NBI, (c) poloidal flux  $\Psi$  contours of the merging ST on the  $R$ - $Z$  plane (lines and colors) for  $V_{PF} = 5.5$  kV and  $I_{tfc} = 80$  kA without NBI.

iment, the produced ST plasma decayed gradually. The merging STs had better confinement, especially just after merging than the single ST, and more than double the plasma current. Note that  $V_{PF} = 6.0$  kV and  $I_{tfc} = 100$  kA are the maximum charging voltage of the PF coils in the flux cores and the external TF coil current that can be applied in the present TS-4 experiments, respectively.

By increasing  $V_{PF}$ , we increased the poloidal flux by more than 50%, but the plasma current dissipated more quickly. In this experiment, the NBI power was not sufficient to sustain the high-beta ST plasma without using the CS coils. However, an ST with poloidal flux greater than 20% was obtained by NBI for  $I_{tfc} = 80$  kA. Because of the tangential beam injection lines on the mid-plane of NBI #1 and #2, as shown in Fig. 1 (b), the NBIs probably contributed considerably to the merging process, i.e., magnetic reconnection, rather than to the formation of the two initial STs.

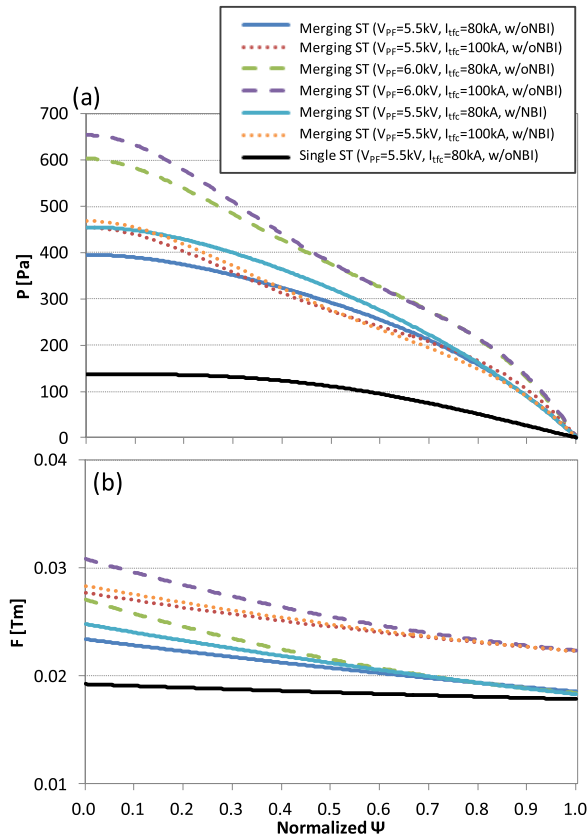


Fig. 4 (a) Plasma thermal pressure  $P(\Psi)$  and (b) poloidal current  $F(\Psi)$  of the merging STs ( $V_{PF} = 5.5/6.0$  kV,  $I_{tfc} = 80/100$  kA, w/wo NBI), and those of the single ST ( $V_{PF} = 5.5$  kV and  $I_{tfc} = 80$  kA without NBI), as a function of normalized poloidal flux at  $t = 410 \mu\text{s}$ .

Figure 4 shows (a) the thermal pressure  $P(\Psi)$  and (b) poloidal current  $F(\Psi)$  of those STs at  $t = 410 \mu\text{s}$  as a function of the poloidal flux  $\Psi$ , where  $P(\Psi)$  and  $F(\Psi)$  were obtained by least-squares fitting of the fourth polynomial expression to the measured profiles assuming of  $P(\Psi_{\text{edge}}) = 0$ . The merging STs had a paramagnetic toroidal field. The thermal pressure and the poloidal current of the produced STs increased with  $V_{PF}$ . The  $P(\Psi)$  profile tends to have a steeper pressure gradient near the magnetic axis at higher  $I_{tfc}$ . As the external toroidal magnetic field because of  $I_{tfc}$ , which corresponds to the guide magnetic field for magnetic reconnection, increases, the ion heating around the downstream region decreases [4]. The pressure gradient of  $P(\Psi)$  probably depends on the ion heating characteristics of the magnetic reconnection.

We observed that NBI increased the plasma pressure of the merging STs by around 10% at  $t = 410 \mu\text{s}$  for  $I_{tfc} = 80$  kA, but quite less for  $I_{tfc} = 100$  kA. This is probably because the trajectories of the fast ions of the two NBIs exhibited better convergence on the  $R$ - $Z$  plane when the external toroidal magnetic field, namely,  $I_{tfc}$ , was increased. We calculated the beam trajectories of the trapped ions using the 2-D ST equilibrium reconstructed

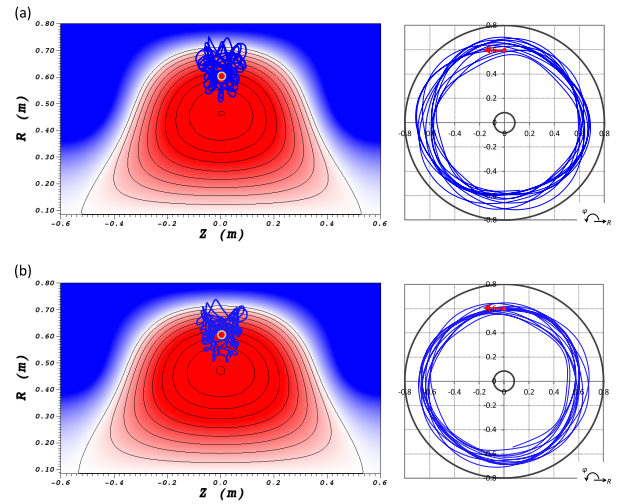


Fig. 5 Beam ion trajectories from the initial position of  $(R, Z) = (0.6 \text{ m}, 0 \text{ m})$  on poloidal (left) and toroidal (right) cross section in the two ST plasma for (a)  $I_{tfc} = 80$  kA and (b) 100 kA under  $V_{PF} = 5.5$  kV during a  $40 \mu\text{s}$  duration. Magnetic flux surfaces used in this calculation are also plotted.

by the Grad-Shafranov equation from the measured profiles shown in Fig. 4 [6]. The ion trajectories were numerically traced by solving the ion motion, including Coulomb collisions with electrons as a form of viscosity. Figure 5 shows the beam ion trajectories from the initial position of  $(R, Z) = (0.6 \text{ m}, 0 \text{ m})$  on the poloidal and toroidal cross sections of the two ST plasma for (a)  $I_{tfc} = 80$  kA and (b) 100 kA under  $V_{PF} = 5.5$  kV. The magnetic flux surfaces used for this calculation are also plotted. The ST plasma with  $I_{tfc} = 80$  kA has a wider ion trajectory than that with  $I_{tfc} = 100$  kA, contributing to the broader absorbed neutral beam power on the magnetic flux surfaces. STs with smaller magnetic fields than those of conventional tokamaks generally have more difficulty in trapping the fast ions injected by NBI. In this experiment, we set the injection positions of NBI #1 and #2 to  $R = 0.6 \text{ m}$  on the basis of the above beam trajectory calculation [7] of the beam trapping rate. As shown in Fig. 3 (c), the major radius of the ST plasma decreases owing to the constant equilibrium field produced by the EF coils. Accordingly, the injection position of the NBIs moved outward, eventually exiting the plasma. Probably because of this effect, NBI for  $I_{tfc} = 100$  kA did not improve the merging ST, indicating that the present setup of TS-4 does not allow NBI to maintain the plasma for longer than  $t \sim 430 \mu\text{s}$ .

### 3. MHD Equilibrium Reconstruction and Pressure-Driven Instability Analysis

The measured profiles of  $P(\Psi)$  and  $F(\Psi)$  at  $t = 410 \mu\text{s}$  shown in Fig. 4 were used to reconstruct their MHD equi-

Table 1 Key plasma parameters for the reconstructed MHD equilibrium of the merging STs produced by  $V_{PF} = 5.5$  or  $6.0$  kV,  $I_{tfc} = 80$  or  $100$  kA without NBI at  $t = 410 \mu\text{s}$ .

	$R_p$ [m]	$A$	$\kappa$	$\delta$	$\beta_t$ [%]	$\beta_p$	$\beta_N$	$I_i$
$V_{PF} = 5.5$ kV, $I_{tfc} = 80$ kA	0.37	1.29	1.42	0.45	34	0.29	5.6	0.21
$V_{PF} = 5.5$ kV, $I_{tfc} = 100$ kA	0.39	1.27	1.32	0.47	27	0.30	5.2	0.25
$V_{PF} = 6.0$ kV, $I_{tfc} = 80$ kA	0.40	1.26	1.31	0.44	54	0.36	8.1	0.30
$V_{PF} = 6.0$ kV, $I_{tfc} = 100$ kA	0.41	1.25	1.32	0.45	40	0.33	6.7	0.30

libria and to evaluate their pressure-driven instabilities (the ideal interchange mode and ideal ballooning mode) using MEUDAS. Here, the merging STs without NBI were selected as targets of the analysis because the results did not show a major difference between operations with and without NBI. Table 1 shows key parameters for the reconstructed MHD equilibria of these STs. The merging STs had a plasma shape of  $R_p \sim 0.4$  m,  $A \sim 1.3$ ,  $\kappa \sim 1.4$  and  $\delta \sim 0.5$ , where  $R_p$  is the major radius,  $A$  is the aspect ratio,  $\kappa$  is the elongation, and  $\delta$  is the triangularity. Because a hollow current profile in the radial direction was formed through magnetic reconnection by colliding two spherical tori [8], the internal plasma inductance of the merging STs was small ( $I_i \sim 0.3$ ). The poloidal beta  $\beta_p$  was around 0.3 owing to the paramagnetic toroidal field of the produced STs. For  $V_{PF} = 6.0$  kV and  $I_{tfc} = 100$  kA, we obtained the highest toroidal beta  $\beta_t$  of greater than 50%, corresponding to a normalized beta  $\beta_N$  of 8.

Figure 6 shows the results of the pressure-driven instability analysis of the reconstructed merging STs. The green area, orange area, and red line indicate the critical pressure gradient ( $\alpha$ ) of the ideal interchange mode, that of the ideal ballooning mode, and the reconstructed equilibrium as a function of the normalized poloidal flux, respectively. The blue line indicates its safety factor  $q$  at the magnetic flux surfaces. We define the critical pressure gradient as that at which one of those growth rates equals zero. If the red line of a certain magnetic surface is within the filled area, it means that the equilibrium is stable against the corresponding mode.

In all cases, the merging STs had weakly reversed shear  $q$  profiles. In two cases,  $V_{PF} = 6.0$  kV (Figs. 6 (c) and (d)), the plasma had a  $q = 1$  magnetic surface near  $|\Psi| = 0.3$  because of the small external toroidal magnetic field compared with the poloidal magnetic field of the two initial STs, suggesting kink instability, which is not considered in this study. The magnetic surfaces with  $q \leq 1$  of these STs are unstable against the ideal interchange mode, and the ideal ballooning mode is also unstable at all magnetic surfaces. We could not easily increase the safety factor by increasing the external toroidal magnetic

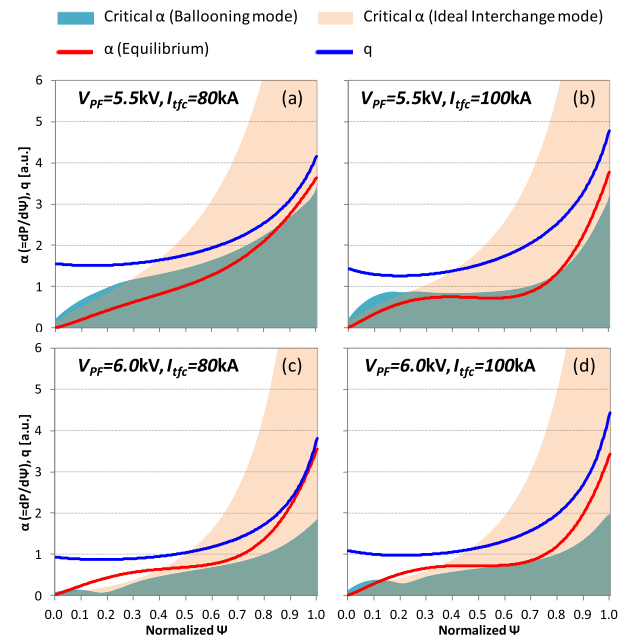


Fig. 6 Pressure-driven instability analysis of the reconstructed merging STs. Green area, orange area, and red line indicate critical pressure gradient ( $\alpha$ ) of the ideal interchange mode, that of the ideal ballooning mode, and reconstructed equilibrium as a function of the normalized poloidal flux, respectively. Blue line indicates its safety factor  $q$  at the magnetic flux surfaces.

field, because it affects both the parameters of the initial STs and the merging process (magnetic reconnection), as mentioned above. In contrast, the magnetic surfaces where  $0.2 \leq |\Psi| \leq 0.7$  approach the ideal ballooning stability limit when  $I_{tfc}$  is increased for  $V_{PF} = 5.5$  kV (Figs. 6 (a) and (b)), owing to the profile variation in  $P(\Psi)$ .

In this analysis, no merging case formed a high-beta ST that was stable against both the ideal interchange mode and the ideal ballooning mode at all the magnetic surfaces. However, we probably overestimated the edge pressure gradient because of the restriction that  $P(\Psi_{edge}) = 0$  in the fitting process of the thermal pressure. Because the

Grad–Shafranov equation is sensitive to the pressure gradient  $dP/d\Psi$ , this restriction may increase the error in the MHD equilibrium reconstruction. A detailed profile measurement is another issue to be improved. It may be possible to obtain the non-inductive start-up of a stable high-beta ST (up to  $\beta_i > 30\%$ ) by the plasma merging method by adjusting the two initial STs, e.g.,  $V_{PF} = 5.5$  kV and  $I_{tfc} = 80$  kA.

#### 4. Summary

In conclusion, we investigated non-inductive ST start-up using the plasma merging method in TS-4 and explored the possibility of a stable high-beta ST ( $\beta_i > 30\%$ ) formation by adjusting the parameters of the initial STs. We precisely analyzed the merging STs by MEUDAS using the experimentally measured profiles and found that they exhibited low-internal inductance, a paramagnetic toroidal field, and weakly reversed shear. Our pressure-driven instability analysis indicated that the STs became unstable against not only the ideal ballooning mode but also the ideal interchange mode when the merging STs had  $q$ -values smaller than 1. The first synchronous NBI exper-

iment, with a total power of 0.4 MW, suggests that NBI mainly contributed to the formation of the two initial STs, i.e., pre-ionization and the merging process, i.e., magnetic reconnection, rather than sustaining and improving the confinement of the produced high-beta STs.

#### Acknowledgment

This research was supported by the Ministry of Education, Science, Sports, and Culture, a Grant-in-Aid from the Japan Society for the Promotion of Science (JSPS) Fellows (24-1756) and a Grant-in-Aid for Scientific Research (A) (No. 22246119).

- [1] Y. Ono *et al.*, 19th IAEA Fusion Energy Conference, EX/P3-15 (2002).
- [2] T. Ii *et al.*, IEEJ Trans. FM **130**, 765 (2010) (in Japanese).
- [3] M. Suzuki *et al.*, JAERI-Data/Code 2001-030 (2001).
- [4] Y. Ono *et al.*, Phys. Rev. Lett. **107**, 185001 (2011).
- [5] T. Ii *et al.*, Rev. Sci. Instrum. **83**, 083504 (2012).
- [6] M. Inomoto *et al.*, Nucl. Fusion **48**, 035013 (2008).
- [7] K. Gi *et al.*, 30th EPS Conf. (Stockholm, Sweden), P4.023 (2012).
- [8] Y. Ono *et al.*, Nucl. Fusion **43**, 789 (2003).